

## Microscopic Approach To Heavy-ion Fusion: role of the Pauli principle

---

**C. Simenel\*, M. Dasgupta, D. J. Hinde**

*Department of Nuclear Physics, Research School of Physics and Engineering, The Australian National University, Canberra ACT 2601, Australia*

*E-mail: [cedric.simenel@anu.edu.au](mailto:cedric.simenel@anu.edu.au)*

**A.S. Umar, K. Godbey**

*Department of Physics and Astronomy, Vanderbilt University, Nashville, TN 37235, USA*

We study the impact of “Pauli repulsion” due to the fermionic nature of the nucleons on heavy-ion fusion . We propose a new microscopic approach, the density-constrained frozen Hartree-Fock method, to compute the bare potential including the Pauli exclusion principle exactly. Pauli repulsion is shown to reduce tunnelling probability and thus contributes to the observed deep sub-barrier fusion hindrance.

*The 26th International Nuclear Physics Conference  
11-16 September, 2016  
Adelaide, Australia*

---

\*Speaker.

The Pauli exclusion principle is known to generate a repulsion (called ‘‘Pauli repulsion’’ hereafter) between nuclei at short distance [1]. The Pauli repulsion should then be included in the nucleus-nucleus potentials used to model reactions such as (in)elastic scattering, (multi)nucleon transfer, and fusion. However, Pauli repulsion is usually neglected in these models: it has been argued that the outcome of a collision between nuclei is mostly determined at a distance where the nuclei do not overlap much and thus the effects of the Pauli exclusion principle are minimized. This argument is based on the assumption that nuclei do not necessarily probe the inner part of the fusion barrier. This argument may not be valid for deep sub-barrier energies where the inner turning-point of the fusion barrier entails significant overlap between the two nuclei [2, 3].

Using a realistic microscopic approach to compute nucleus-nucleus bare potentials, we show that, in fact, the Pauli repulsion plays an important role on fusion at deep sub-barrier energies. In particular, it provides a natural (though only partial) explanation for the experimentally observed deep sub-barrier fusion hindrance [4, 5, 6] (see Ref. [7] for a review). Various theoretical explanations have been proposed to explain this effect [8, 9, 5, 10, 11, 12, 13]. However, none of them directly consider Pauli repulsion as a possible mechanism.

In order to investigate the effect of Pauli repulsion on heavy-ion fusion, we introduce a novel microscopic method called density-constrained frozen Hartree-Fock (DCFHF) to compute the interaction between nuclei while accounting exactly for the Pauli exclusion principle between nucleons. The microscopically derived bare nucleus-nucleus potential including Pauli repulsion is then used to study deep sub-barrier fusion. For simplicity, we focus on systems with doubly-magic nuclei which are spherical and non-superfluid:  $^{16}\text{O}+^{16}\text{O}$ ,  $^{40,48}\text{Ca}+^{40,48}\text{Ca}$ ,  $^{16}\text{O}+^{208}\text{Pb}$ , and  $^{48}\text{Ca}+^{208}\text{Pb}$ .

To avoid the introduction of new parameters, we adopt the idea of Brueckner *et al.* [14] to derive the bare potential from an energy density functional (EDF)  $E[\rho]$  written as an integral of an energy density  $\mathcal{H}[\rho(\mathbf{r})]$ , i.e.,

$$E[\rho] = \int d\mathbf{r} \mathcal{H}[\rho(\mathbf{r})]. \quad (1)$$

The bare potential is obtained by requiring frozen ground-state densities  $\rho_i$  of each nucleus ( $i = 1, 2$ ) which we compute using the Hartree-Fock (HF) mean-field approximation [15, 16]. The Skyrme EDF [17] is used both in HF calculations and to compute the bare potential. It accounts for the bulk properties of nuclear matter such as its incompressibility which is crucial at short distances [14, 8, 18]. Neglecting the Pauli exclusion principle between nucleons in different nuclei leads to the usual frozen Hartree-Fock (FHF) potential [19, 20, 21, 22]

$$V_{FHF}(\mathbf{R}) = \int d\mathbf{r} \mathcal{H}[\rho_1(\mathbf{r}) + \rho_2(\mathbf{r} - \mathbf{R})] - E[\rho_1] - E[\rho_2], \quad (2)$$

where  $\mathbf{R}$  is the distance vector between the centres of mass of the nuclei. The FHF potential, assumed to be central, can then directly be used to compute fusion cross-sections [23, 24, 25].

Our new DCFHF method is the static counter-part of the density-constrained time-dependent Hartree-Fock approach developed to extract the nucleus-nucleus potential of dynamically evolving systems [26]. In particular, this approach shows that the Pauli exclusion principle splits orbitals such that some states contribute attractively (bounding) and some repulsively (antibounding) to the potential [27]. In order to disentangle effects of the Pauli exclusion principle from the dynamics,

we need to investigate the bare potential without polarisation effects. The dynamics can be included in a second step via, e.g., coupled-channels [23] or TDHF [20, 28, 29] calculations.

In the present method, it is important that the nuclear densities remain frozen as the densities of the HF ground-states of the collision partners. Consequently, the DCFHF approach facilitates the computation of the bare potential by using the self-consistent HF mean-field with exact frozen densities. The Pauli exclusion principle is included exactly by allowing the single-particle states, comprising the combined nuclear density, to reorganize to attain their minimum energy configuration and be properly antisymmetrized as the many-body state is a Slater determinant of all the occupied single-particle wave-functions. The HF minimization of the combined system is thus performed subject to the constraint that the local proton ( $p$ ) and neutron ( $n$ ) densities do not change:

$$\delta \langle H - \sum_{q=p,n} \int d\mathbf{r} \lambda_q(\mathbf{r}) [\rho_{1_q}(\mathbf{r}) + \rho_{2_q}(\mathbf{r} - \mathbf{R})] \rangle = 0, \quad (3)$$

where the  $\lambda_{n,p}(\mathbf{r})$  are Lagrange parameters at each point of space constraining the neutron and proton densities. This equation determines the state vector (Slater determinant)  $|\Phi(\mathbf{R})\rangle$ . The DCFHF potential, assumed to be central, is then defined as

$$V_{\text{DCFHF}}(R) = \langle \Phi(\mathbf{R}) | H | \Phi(\mathbf{R}) \rangle - E[\rho_1] - E[\rho_2]. \quad (4)$$

FHF and DCFHF calculations of bare nucleus-nucleus potentials were done in a three-dimensional Cartesian geometry with no symmetry assumptions using a static version of the code of Ref. [30] and using the Skyrme SLy4d interaction [31] which has been successful in describing various types of nuclear reactions [22]. The three-dimensional Poisson equation for the Coulomb potential is solved by using Fast-Fourier Transform techniques and the Slater approximation is used for the Coulomb exchange term. The static HF equations and the DCFHF minimizations are implemented using the damped gradient iteration method. The box size used for all the calculations was chosen to be  $60 \times 30 \times 30 \text{ fm}^3$ , with a mesh spacing of 1.0 fm in all directions. These values provide very accurate results due to the employment of sophisticated discretization techniques [32, 33].

The FHF (solid line) and DCFHF (dashed line) potentials are shown in Figs. 1(a-c) for  $^{40}\text{Ca}+^{40}\text{Ca}$ ,  $^{48}\text{Ca}+^{48}\text{Ca}$ , and  $^{16}\text{O}+^{208}\text{Pb}$  systems, respectively. Potentials for  $^{16}\text{O}+^{16}\text{O}$ ,  $^{40}\text{Ca}+^{48}\text{Ca}$  and  $^{48}\text{Ca}+^{208}\text{Pb}$  are also shown in Fig. 2, 3 and 4, respectively. We observe that the Pauli exclusion principle (present only in DCFHF) induces a repulsion at short distance in the three systems. The resulting effects are negligible outside the barrier and relatively modest near the barrier. However, the impact is more important in the inner barrier region, with the production of a potential pocket at short distance. In  $^{16}\text{O}+^{16}\text{O}$ , Pauli repulsion is small and near the barrier. It only becomes significant at very low-energy. Pauli repulsion could therefore have an impact at astrophysical energies.

We also see that the effect of Pauli repulsion increases for systems with large charge products  $Z_1 Z_2$ . Indeed the DCFHF potential pocket almost disappears in  $^{48}\text{Ca}+^{208}\text{Pb}$ . However, the two-body picture for such heavy systems is questionable. Fig. 4 shows indeed an extreme case where the DCFHF calculation predicts that fusion is impossible at 3% below the barrier. In fact, a smooth transition toward an adiabatic potential for the compound system is expected [12] which would allow fusion to occur at lower energies.

Finally, Fig. 3 shows that the Pauli repulsion not only depends on  $Z_1 Z_2$ , but also on the number of neutrons. At touching distance, additional neutrons increase the barrier radius (due to the

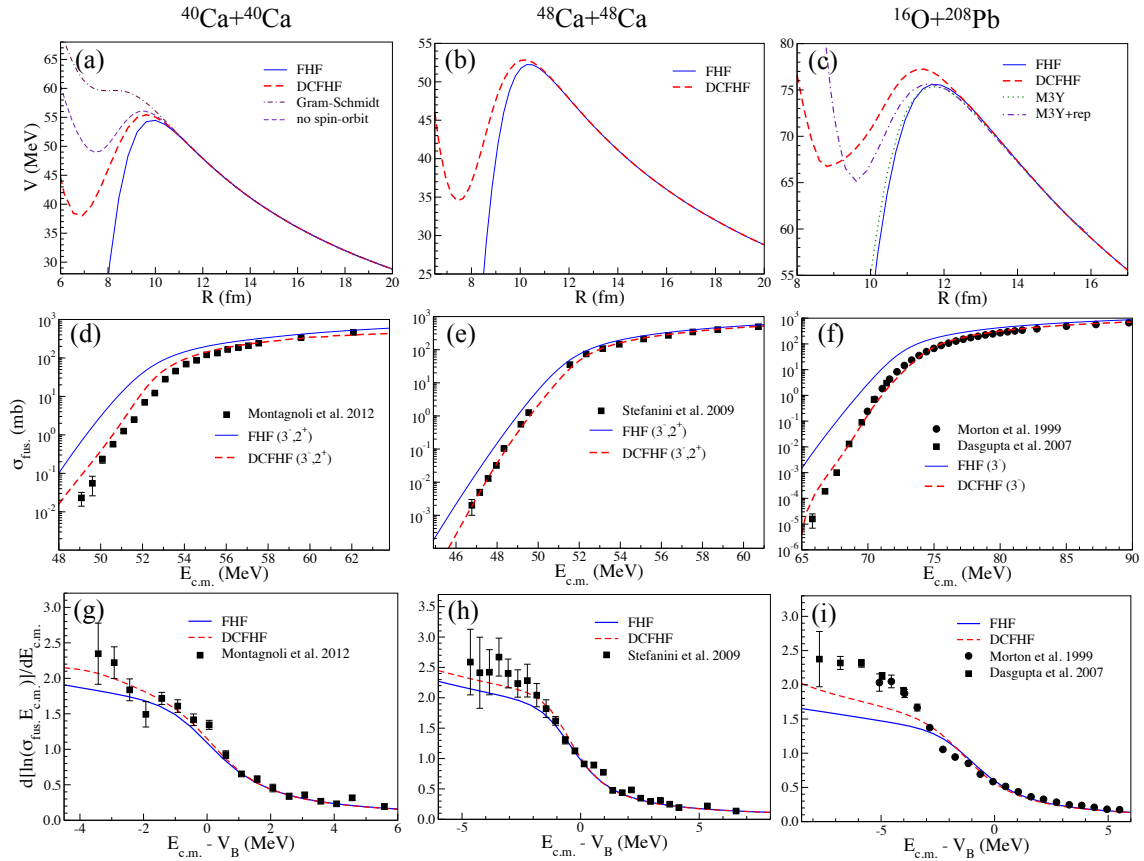


**Figure 1:** (Color online) (a-c) Nucleus-nucleus potential without (FHF) and with (DCFHF) Pauli exclusion principle between nucleons of different nuclei. Potentials from a Gram-Schmidt antisymmetrization (dotted-dashed line) and from DCFHF without rearrangement of the spin-orbit density (thin dashed line) are shown in panel (a). M3Y (dotted line) and M3Y+rep (dotted-dashed line) phenomenological potentials [34] are shown in panel (c). (d-f) Experimental [35, 5, 36, 37] and theoretical (coupled-channels calculations with couplings to low-lying collective  $2^+$  and/or  $3^-$  states) fusion cross-sections  $\sigma_{fus}$  versus centre of mass energy  $E_{c.m.}$ . (g-i) Logarithmic slopes of  $\sigma_{fus} \cdot E_{c.m.}$  versus  $E_{c.m.} - V_B$  where  $V_B$  is the barrier energy. In (g-i), FHF and DCFHF cross-sections are obtained without couplings, the latter being included via a shift in  $E_{c.m.}$  (see text).

neutron skin) and thus increase its height. For this reason,  $^{48}\text{Ca}+^{48}\text{Ca}$  has the lowest barrier and  $^{40}\text{Ca}+^{40}\text{Ca}$  the largest one. However,  $^{48}\text{Ca}+^{48}\text{Ca}$  also exhibits the strongest Pauli repulsion of the three systems. This is interpreted as an effect of the larger number of neutrons overlapping at short distance, thus increasing the Pauli repulsion.

The most important effect of Pauli repulsion is to increase the barrier width. It is then expected to reduce the sub-barrier tunneling probability as the latter decreases exponentially with the barrier width.

Coupled-channels calculations of fusion cross-sections were performed with the CCFULL code [38] using Woods-Saxon fits of the FHF and DCFHF potentials. By default, the incoming wave boundary condition (IWBC) was used. For shallow pocket potentials, however, the IWBC should be replaced by an imaginary potential at the potential pocket to avoid numerical instabilities. This

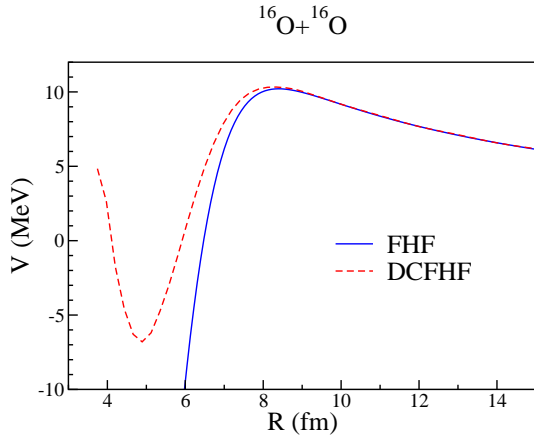


**Figure 2:** (Color online) Nucleus-nucleus potential for the  $^{16}\text{O}+^{16}\text{O}$  system without (FHF) and with (DCFHF) Pauli exclusion principle between nucleons of different nuclei.

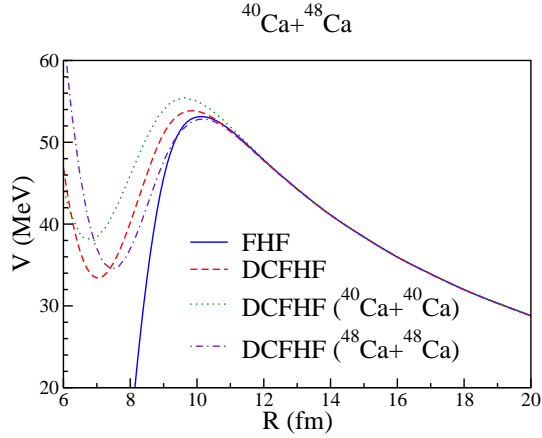


**Figure 3:** (Color online) Same as Fig. 2 for the  $^{40}\text{Ca}+^{48}\text{Ca}$  system. DCFHF potentials for  $^{40}\text{Ca}+^{40}\text{Ca}$  and  $^{48}\text{Ca}+^{48}\text{Ca}$  are also shown.

is done for calculations with the  $^{16}\text{O}+^{208}\text{Pb}$  DCFHF potential using a modified version of CCFULL with Woods-Saxon parameters  $\{V_I = 30 \text{ MeV}, a_I = 1 \text{ fm}, r_I = 0.3 \text{ fm}\}$  for the imaginary potential. Couplings to the low-lying collective  $2^+$  (in calcium isotopes) and  $3^-$  states are included with standard values of the coupling constants [35, 39]. In CCFULL, one (two) vibrational mode(s) can be included in the projectile (target). For the  $2^+$  states, we then use the fact that, for symmetric systems, the mutual excitation of one-phonon states in both nuclei can be approximated by one phonon with a coupling constant scaled by  $\sqrt{2}$  [40]. Here, the CC calculations are kept simple and include only the most relevant couplings. Improvements could be obtained, e.g., by including anharmonicity of the multi-phonon states [41]. The resulting fusion cross-sections are plotted in Figs. 1(d-f). Calculations with the FHF potential systematically overestimate the data while the DCFHF potential leads to a much better agreement with experiment at all energies, and ranging over eight orders of magnitude in cross-sections. This shows the importance of taking into account

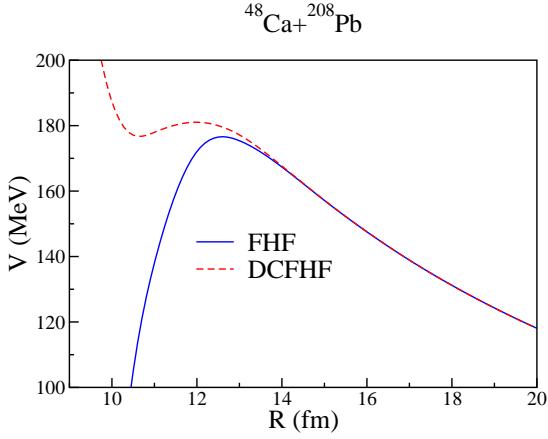


**Figure 4:** (Color online) Same as Fig. 2 for the  $^{48}\text{Ca}+^{208}\text{Pb}$  system.

Pauli repulsion in the bare potential for fusion calculations. We emphasise that these calculations are performed without adjustable parameters.

The behaviour of fusion at deep sub-barrier energies is often studied using the logarithmic slope  $d\ln(\sigma_{fus}.E_{c.m.})/dE_{c.m.}$ . Large logarithmic slopes are a signature of a rapid decrease of  $\sigma_{fus.}$  with decreasing energy. Deep-sub-barrier fusion hindrance is characterised by the failure of theoretical models to reproduce large logarithmic slopes observed experimentally at low energy. To avoid numerical instabilities due to shallow potentials in the calculations of logarithmic slopes, couplings to internal excitations of the nuclei have been removed in the calculations of barrier transmission and accounted for via an overall lowering of  $V_B$  by less than 5% depending on the structure of the reactants [5]. Indeed, it has been shown that couplings have little effects on the logarithmic slope at these energies [5]. We see in Fig. 1(g-i) that the inclusion of Pauli repulsion in DCFHF indeed increases the logarithmic slope at low energy. Although Pauli repulsion is shown to play a crucial role, it is not yet sufficient to reproduce experimental data at deep sub-barrier energies. Other contributions are expected to come from dissipative effects [5] and from the transition between the nucleus-nucleus potential to the one-nucleus adiabatic potential [12]. However, repulsive effects from the incompressibility of nuclear matter invoked in [8] are not observed in our microscopic calculations. Both the FHF and DCFHF calculations use the same Skyrme functional (SLy4d) with a realistic compression modulus of the symmetric nuclear matter  $K_\infty \simeq 230$  MeV. Although the FHF potential properly takes into account effects due to incompressibility, it is very close to standard phenomenological potentials. We illustrate this with the example of the M3Y potential [8] in Fig. 1(c). The addition of a repulsive component at short distance [M3Y+rep parametrisation shown with a dotted-dashed line Fig. 1(c)], introduced phenomenologically in [8] to explain experimental fusion data at deep sub-barrier energies, then cannot be justified by an effect of incompressibility. It is more likely that it simulates other effects such as Pauli repulsion.

C.S. thanks E. Simpson for useful discussions. This work has been supported by the Australian Research Council Grant No. FT120100760, and by the U.S. Department of Energy under grant No. DE-SC0013847 with Vanderbilt University.

## References

- [1] T. Fließbach, *Z. Phys.* **247**, 117 (1971).
- [2] C. H. Dasso and G. Pollaro, *Phys. Rev. C* **68**, 054604 (2003).
- [3] A. S. Umar, V. E. Oberacker, and C. J. Horowitz, *Phys. Rev. C* **85**, 055801 (2012a).
- [4] C. L. Jiang, H. Esbensen, K. E. Rehm, B. B. Back, R. V. F. Janssens, J. A. Caggiano, P. Collon, J. Greene, A. M. Heinz, D. J. Henderson, I. Nishinaka, T. O. Pennington, and D. Seweryniak, *Phys. Rev. Lett.* **89**, 052701 (2002).
- [5] M. Dasgupta, D. J. Hinde, A. Diaz-Torres, B. Bouriquet, C. I. Low, G. J. Milburn, and J. O. Newton, *Phys. Rev. Lett.* **99**, 192701 (2007).
- [6] A. M. Stefanini, G. Montagnoli, L. Corradi, S. Courtin, E. Fioretto, A. Goasduff, F. Haas, P. Mason, R. Silvestri, P. P. Singh, F. Scarlassara, and S. Szilner, *Phys. Rev. C* **82**, 014614 (2010).
- [7] B. B. Back, H. Esbensen, C. L. Jiang, and K. E. Rehm, *Rev. Mod. Phys.* **86**, 317 (2014).
- [8] Ş. Mişicu and H. Esbensen, *Phys. Rev. Lett.* **96**, 112701 (2006).
- [9] Ş. Mişicu and H. Esbensen, *Phys. Rev. C* **75**, 034606 (2007).
- [10] A. Diaz-Torres, D. J. Hinde, M. Dasgupta, G. J. Milburn, and J. A. Tostevin, *Phys. Rev. C* **78**, 064604 (2008).
- [11] A. Diaz-Torres, *Phys. Rev. C* **82**, 054617 (2010).
- [12] Takatoshi Ichikawa, Kouichi Hagino, and Akira Iwamoto, *Phys. Rev. Lett.* **103**, 202701 (2009).
- [13] T. Ichikawa, *Phys. Rev. C* **92**, 064604 (2015).
- [14] K. A. Brueckner, J. R. Buchler, and M. M. Kelly, *Phys. Rev.* **173**, 944 (1968).
- [15] D. R. Hartree, *Proc. Camb. Phil. Soc.* **24**, 89 (1928).
- [16] V. A. Fock, *Z. Phys.* **61**, 126 (1930).
- [17] T. H. R. Skyrme, *Phil. Mag.* **1**, 1043 (1956).
- [18] S. Hossain, A. S. B. Tariq, A. Nilima, M. S. Islam, R. Majumder, M. A. Sayed, M. M. Billah, M. M. B. Azad, M. A. Uddin, I. Reichstein, F. B. Malik, and A. K. Basak, *Phys. Rev. C* **91**, 064613 (2015).
- [19] V. Y. Denisov and W. Nörenberg, *Eur. Phys. J. A* **15**, 375 (2002).
- [20] Kouhei Washiyama and Denis Lacroix, *Phys. Rev. C* **78**, 024610 (2008).
- [21] Cédric Simenel and Benoit Avez, *Intl. J. Mod. Phys. E* **17**, 31 (2008).
- [22] C. Simenel, *Eur. Phys. J. A* **48**, 152 (2012).
- [23] C. Simenel, M. Dasgupta, D. J. Hinde, and E. Williams, *Phys. Rev. C* **88**, 064604 (2013a).
- [24] D. Bourgin, C. Simenel, S. Courtin, and F. Haas, *Phys. Rev. C* **93**, 034604 (2016).
- [25] K. Vo-Phuoc, C. Simenel, and E. C. Simpson, *Phys. Rev. C* **94**, 024612 (2016).
- [26] A. S. Umar and V. E. Oberacker, *Phys. Rev. C* **74**, 021601 (2006a).
- [27] A. S. Umar, V. E. Oberacker, J. A. Maruhn, and P.-G. Reinhard, *Phys. Rev. C* **85**, 017602 (2012b).
- [28] C. Simenel, R. Keser, A. S. Umar, and V. E. Oberacker, *Phys. Rev. C* **88**, 024617 (2013b).

- [29] A. S. Umar, C. Simenel, and V. E. Oberacker, *Phys. Rev. C* **89**, 034611 (2014).
- [30] A. S. Umar and V. E. Oberacker, *Phys. Rev. C* **73**, 054607 (2006b).
- [31] Ka-Hae Kim, Takaharu Otsuka, and Paul Bonche, *J. Phys. G* **23**, 1267 (1997).
- [32] A. S. Umar, M. R. Strayer, J. S. Wu, D. J. Dean, and M. C. Güçlü, *Phys. Rev. C* **44**, 2512 (1991a).
- [33] A. S. Umar, J. Wu, M. R. Strayer, and C. Bottcher, *J. Comp. Phys.* **93**, 426 (1991b).
- [34] Henning Esbensen and Şerban Mişicu, *Phys. Rev. C* **76**, 054609 (2007).
- [35] C. R. Morton, A. C. Berriman, M. Dasgupta, D. J. Hinde, J. O. Newton, K. Hagino, and I. J. Thompson, *Phys. Rev. C* **60**, 044608 (1999).
- [36] G. Montagnoli, A. M. Stefanini, C. L. Jiang, H. Esbensen, L. Corradi, S. Courtin, E. Fioretto, A. Goasduff, F. Haas, A. F. Kifle, C. Michelagnoli, D. Montanari, T. Mijatović, K. E. Rehm, R. Silvestri, P. P. Singh, F. Scarlassara, S. Szilner, X. D. Tang, and C. A. Ur, *Phys. Rev. C* **85**, 024607 (2012).
- [37] A. M. Stefanini, G. Montagnoli, R. Silvestri, L. Corradi, S. Courtin, E. Fioretto, B. Guiot, F. Haas, D. Lebhertz, P. Mason, F. Scarlassara, and S. Szilner, *Phys. Lett. B* **679**, 95 (2009).
- [38] K. Hagino, N. Rowley, and A. Kruppa, *Comput. Phys. Commun.* **123**, 143 (1999).
- [39] N. Rowley and K. Hagino, *Nucl. Phys. A* **834**, 110c (2010).
- [40] H. Esbensen and S. Landowne, *Phys. Rev. C* **35**, 2090 (1987).
- [41] J. M. Yao and K. Hagino, *Phys. Rev. C* **94**, 011303 (2016).